

Received: 2017.03.18  
Accepted: 2017.08.10  
Published: 2018.03.02

# Preoperative Computed Tomography (CT) Evaluation of Anatomical Abnormalities in Endonasal Transsphenoidal Approach in Pituitary Adenoma

1 Taian City Central Hospital, Taian, Shandong, P.R. China  
2 Taishan Medical University, Taian, Shandong, P.R. China

Authors' Contribution:  
Study Design A  
Data Collection B  
Statistical Analysis C  
Data Interpretation D  
Manuscript Preparation E  
Literature Search F  
Funds Collection G

BE 1 **Zhengyi Guo\***  
CF 1 **Chunli Liu\***  
F 2 **Haifeng Hou\***  
D 1 **Ruiying Li**  
D 1 **Jichun Su**  
C 1 **Fuyong Zhang**  
CE 1 **Guoqiang Xing**  
B 1 **Linlin Qian**  
G 2 **Jianfeng Qiu**  
AE 1 **Yuanzhong Xie**  
AE 1 **Ningxi Zhu**

\* These authors contributed equally to this work

**Corresponding Authors:**  
**Source of support:**

Ningxi Zhu, e-mail: [zhuningxi28@163.com](mailto:zhuningxi28@163.com), Yuanzhong Xie, e-mail: [xie01088@126.com](mailto:xie01088@126.com)  
This study was supported by the China National Key Research and Development Program (2016YFC0103400)

**Background:** This study aimed to retrospectively analyze patient clinical data to investigate the effects of computed tomography (CT) reconstruction and the measurement of abnormal structures in the endonasal sphenoidal sinus approach on the operative effects in patients undergoing pituitary adenoma resection.





**Material/Methods:** The records of 53 patients who underwent pituitary adenoma resection via the endonasal transsphenoidal approach in the Neurosurgery Department of Tai'an City Central Hospital from December 2010 to June 2016 were analyzed retrospectively. All cases showed anatomical abnormalities in the endonasal transsphenoidal approach that were detected by conventional CT scans. The clinical data of the patients were reviewed. After review, 26 patients who underwent preoperative CT reconstruction and measurement of abnormal structures before surgery were included in the observation group (CT reconstruction group), and 27 patients who did not undergo CT reconstruction and measurement of abnormal structures were included in the control group. Data on intraoperative blood loss, surgical time, hospital stay, and postoperative complications were collected to assess the quality of the surgery.

**Results:** Compared with the control group, the observation group showed less blood loss ( $p < 0.001$ ), a shorter operation time ( $p < 0.001$ ), fewer postoperative complications ( $p < 0.001$ ), and a shorter hospital stay ( $p < 0.001$ ).

**Conclusions:** Preoperative CT reconstruction and measurement of abnormal structures in patients undergoing pituitary adenoma resection by the endonasal transsphenoidal approach can improve operative quality and reduce complications.

**MeSH Keywords:** **Alendronate • Neuronal Tract-Tracers • Pituitary Neoplasms • Tomography Scanners, X-Ray Computed**

**Full-text PDF:** <https://www.medscimonit.com/abstract/index/idArt/904402>

 2081  4  4  38



## Background

Since pituitary adenoma resection using the endonasal transsphenoidal approach was established in 1969 [1], it has been the first choice for surgical treatment of pituitary adenoma [2–4]. Recently, an endoscopic endonasal transsphenoidal approach for the treatment of pituitary adenoma, which conforms to the trends in development of micro-invasive technology, was determined to be a safe and effective clinical therapeutic method with fewer complications, and thus was successfully recommended [5–7]. At present, scholars have conducted several studies on tumor resection and its postoperative complications, but few have focused on the effects of anatomical variations in the endonasal transsphenoidal approach on surgical outcomes [8–12]. As a result, poor endoscopic access, increased intraoperative blood loss, and delayed surgical time often occurred during surgery [13]. Prior to the availability of computed tomography/magnetic resonance imaging (CT/MRI) navigation, and the application of CT multiplanar reconstruction (MPR) and three-dimensional (3D) reconstruction with accurate measurements of lumen diameters and angles in the sphenoidal region prior to surgery, the use of the surgical microscope could achieve safety and success, with fewer complications and with precise positioning [14,15]. Consistent CT reconstruction prior to surgery with intraoperative microscopic structural imaging could achieve the purpose of image-guided surgery.

## Material and Methods

### Subjects

The records of patients with pituitary adenoma in the saddle area admitted to our hospital from December 2010 to June 2016 were retrospectively investigated. Inclusion criteria were: (1) presence of anatomical abnormalities in the endonasal transsphenoidal approach detected by CT, (2) completion of the surgery, and (3) the availability of sufficient clinical data for our study. Exclusion criteria were the presence of inflammation of the nasal cavity, polyps, or a history of tumor. All patients who were included in the study provided informed consent, and the study was approved by the Ethics Committee of Tai'an City Central Hospital.

After reviewing the clinical data, 26 patients who underwent preoperative CT reconstruction and measurement of abnormal structures were included in the observation group (CT reconstruction group), and 27 patients who did not undergo CT reconstruction and measurement were included in the control group. The observation group included 12 men and 14 women ranging in age from 23 to 76 (mean age, 45.6). The control group included 14 men and 13 women ranging in age from 26 to 74 (mean age, 47.2) years.

### Data collection

Preoperative imaging data were obtained from the original data in the CT workstation. Before surgery, all 53 patients underwent thinner scanning of the area from the upper margin of the frontal sinus to the lower margin of the mandible with a layer thickness of 0.625 mm using a 128 spiral CT scanner (Syngo MMWP, Siemens, Germany) in skeletal algorithm imaging and the data were recorded in the workstation.

Before surgery in the observation group, a workstation was used to obtain sequential transverse, coronal, and sagittal images of the structures in the nasal cavity, including the positions and morphology of the nasal septum, middle turbinate pneumatization, middle turbinate reverse bending, the sphenoid sinus, the sphenoid fissure, conchal sphenoid pneumatization, the relationship between the sphenoid sinus and internal carotid artery, and any bone defects. The images were reconstructed and printed for use during surgery. The control group did not undergo CT reconstruction of the above anatomical structures.

Before surgery, the images were studied and possible problems were assessed. Pituitary adenoma resection was performed using an approach through a unilateral nostril, the middle meatus, the sphenoid sinus, and the floor of the sella using an operating microscope (M525MS3; Leica, Germany).

Surgical complications, operation time, blood loss, hospital stay, and other data were obtained from the medical records of all 53 patients.

### Statistical analysis

Statistical analysis was performed using SPSS 20.0 statistics (IBM Corp., Armonk, NY, USA). The imaging measurements, intraoperative blood loss, operation time, and postoperative hospital stay are expressed as mean  $\pm$ SD. The mean differences between the 2 groups were compared using the *t* test. The category data of the anatomical abnormalities, postoperative complications, and other data are expressed as a constituent ratio or rate and were compared using the chi-square ( $\chi^2$ ) test.  $P < 0.05$  was considered significant.

## Results

### The baseline characteristics of the subjects

Characteristics such as age, sex, and tumor pathological type, size, and resection rate are shown in Table 1. These characteristics were not significantly different between the observation group and the control group ( $p > 0.05$ ), and the groups were therefore comparable.

**Table 1.** Baseline characteristics of subjects.

Items	Observation group (n=26)	Control group (n=27)	P values	
Demographics	Age	45.6±7.4	0.504	
	Men	12	14	0.678
Tumor pathological type	Prolactin cell adenoma	12	11	0.691
	Growth hormone adenoma	3	4	1.000*
	ACTH cell adenoma	2	3	1.000*
	TSH adenoma	1	2	1.000*
	non-secretory adenoma	8	7	0.484
	<1	2	3	0.747
Tumor size (cm)	1–4	16	18	
	≥4	8	6	
	Total resection	20	21	0.941
Tumor resection rate	Subtotal resection	6	6	

\* Was calculated using continuity correction. ACTH – Adrenocorticotropic hormone; TSH – thyroid stimulating hormone

**Anatomical abnormalities and image reconstruction**

Figure 1 shows head CT angiogram (CTA) MPR images of internal carotid artery bone defects in the lumen of the sphenoidal sinus of a patient. From multi-slice images of the cross-sectional, sagittal, and coronal planes, the left internal carotid artery exposed to the lumen of the sphenoidal sinus due to bone defects is visible. The MPR image analysis was performed in typical patients showing anatomical abnormalities in the endonasal transsphenoidal approach (Figure 2). The anatomical abnormalities included a nasal septum curve to the left, significant bilateral middle turbinate gasification, and bilateral outward middle turbinate curve (Figure 2A–2C). Multi-slice images of cross-sectional, coronal planes, and sagittal views (Figure 2D–2F) show the abnormal course of the optic nerve to the ethmoid above the sphenoid sinus. Figure 2G and 2H show either poor or excess pneumatization of the sphenoid sinus.

Anatomical characteristics of the 53 patients are shown in Table 2. The incidences of various anatomical abnormalities in the observation group were: 6 (23.1%) with nasal septal curve to the left, 5 (19.2%) with bilateral middle turbinate pneumatization, 2 (7.7%) with bilateral outward middle turbinate curvature, 1 (3.8%) with ethmoid sinus above the sphenoid sinus, 1 (3.8%) with vertical sphenoid fissure (Figure 3A), 0 with poor conchal sphenoid pneumatization, 0 with the interval of sphenoid sinus, and 1 (3.7%) with internal carotid artery bone defects. The observation and control groups were compared using the  $\chi^2$  test; the results showed there was no

significant difference in anatomical abnormalities between the 2 groups ( $p>0.05$ ).

**3-D reconstruction and MPR measurement of the lumen of the nasal sphenoidal region in the observation group**

3-D reconstruction and MPR measurement of the lumen in the nasal sphenoidal region are shown in Figure 3. Figure 3B–3E show 3-D reconstructed images of an abnormal single sphenoidal septum (central, left-of-center, right-of-center, and slanting) and multi-atrial sphenoidal septum (Figure 3F). Figure 4 shows the MPR measurement of the lumen of the nasal sphenoidal region; the OM distance [between the columella root (point O) and the sphenoidal sinus inferior pole (point M)] is  $69.87\pm5.23$  mm. The elevation angle MOL formed by the connection between the Aeby’s plane (L) and the OM was  $31.07\pm6.40$  degrees. The distance between point M and sellar floor midpoint P was  $13.15\pm1.68$  mm. The thickness of the sellar floor was  $2.13\pm1.85$  mm. The MPR anteroposterior diameter of the sphenoidal sinus was  $25.9\pm6.0$  mm, the left to right diameter was  $37.3\pm7.0$  mm, and the vertical diameter was  $26.4\pm4.8$  mm.

**Postoperative complications**

The incidence of postoperative complications in all patients is shown in Table 3. Cerebrospinal fluid leakage occurred most frequently, with 1 case in the observation group (3.8%, 1/26) and 4 cases in the control group (14.8%, 4/27). Intracranial infection occurred least frequently, with 0 cases in the observation

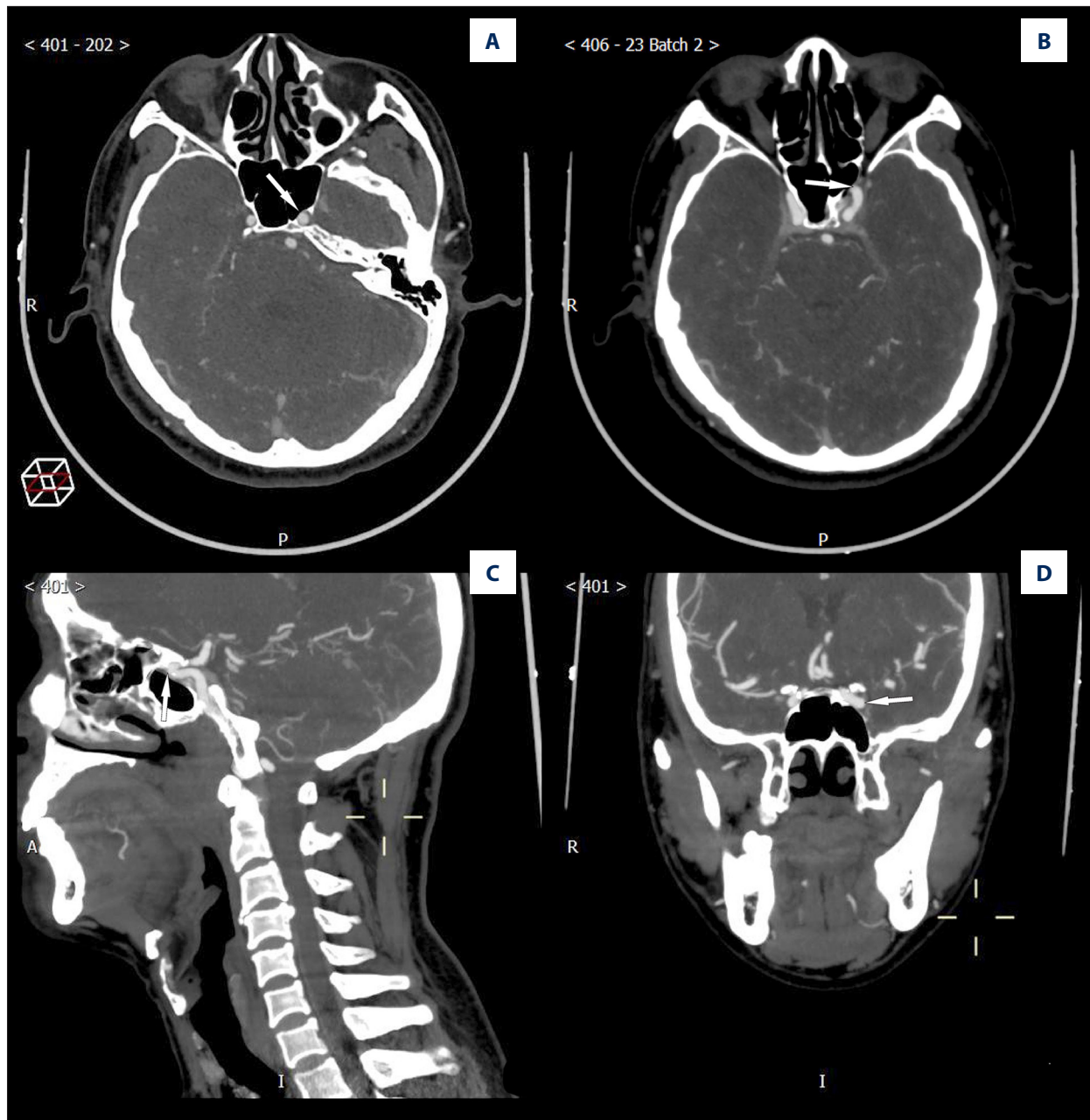


**Figure 1.** Multiplanar reconstruction (MPR) of head computed tomography angiogram images of the internal carotid artery bone defects in the lumen of the sphenoidal sinus in a patient. **(A)** Axial image of the internal carotid artery in the lateral wall of the sphenoid sinus. The arrows indicate a bone defect on the left; there is no bone defect on the right. **(B)** Axial image of the internal carotid artery at the front and rear along the lateral wall of the sphenoid sinus. The arrows indicate a bone defect on the left; there is no bone defect on the right. **(C)** MPR sagittal image of the internal carotid artery exposed to the lumen of the sphenoidal sinus due to bone defects, as indicated by the arrows. **(D)** MPR coronal images of the left and right internal carotid arteries. The arrows indicate a bone defect in the left lumen of the sphenoidal sinus.

group and 1 case in the control group (3.7%, 1/27). The difference between the 2 groups was statistically significant ( $p < 0.05$ ), as seen in Table 3.

#### Perioperative indexes

By comparing the postoperative hospital stay, intraoperative blood loss, and operation time between the 2 groups, we observed that the indexes were significantly lower in the

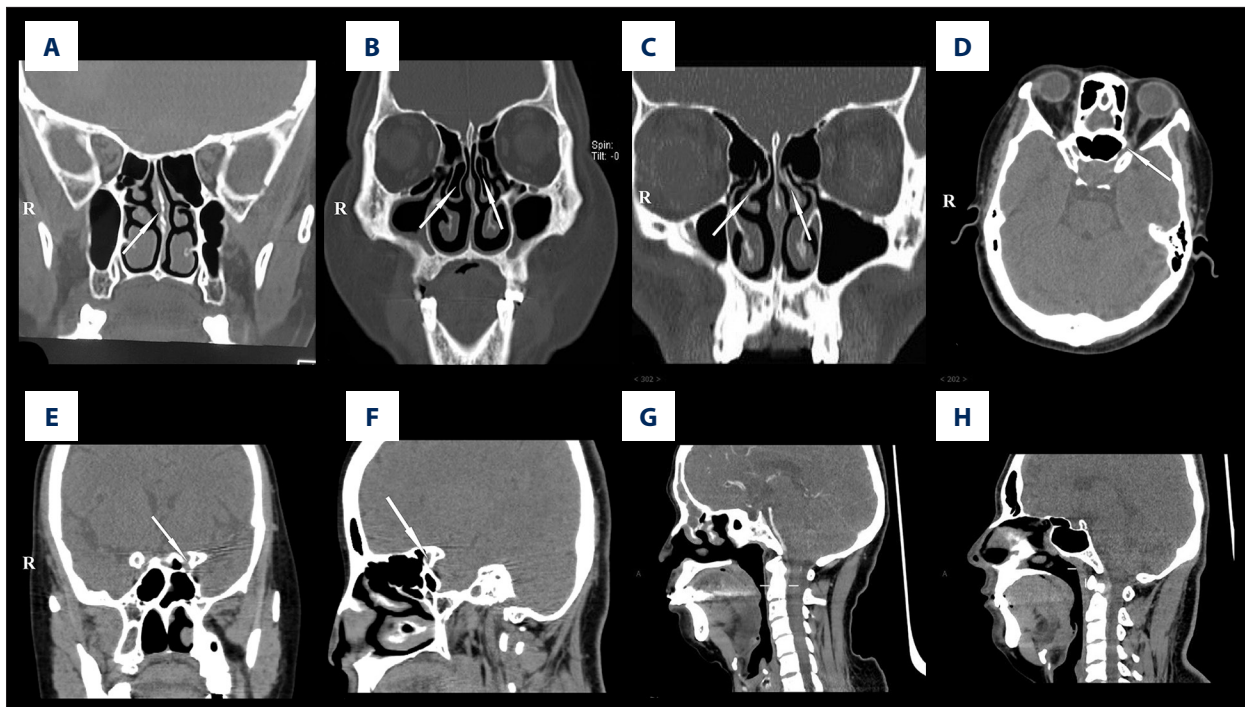


**Figure 2.** Multiplanar reconstruction (MPR) images of anatomical abnormalities in the endonasal transsphenoidal approach in typical patients. The arrows indicate (A) nasal septum curve to the left, (B) bilateral middle turbinate gasification, (C) bilateral middle turbinate curve reverse, and (D) bilateral ethmoid sinus above the sphenoid sinus. (E) Sphenoidal sinus gasification of the conchal type. (F) Sphenoidal sinus gasification of the saddle pillow type.

**Table 2.** Abnormal anatomical distribution in the observation group and the control group [number (%)].

Groups	Cases	Nasal septum curve	Middle turbinate gasification	Middle turbinate curve reverse	Ethmoid sinus above the sphenoid sinus	Fissured sphenoid sinus	Sphenoidal sinus gasification of conchiform type	Multi-atrial septum of sphenoidal sinus	Internal carotid artery bone defects
Observation group	26	6 (23.1)	5 (19.2)	2 (7.7)	1 (3.8)	1 (3.8)	1 (3.8)	1 (3.8)	1 (3.7)
Control group	27	5 (18.5)	4 (14.8)	1 (3.7)	2 (7.4)	2 (7.4)	0	0	0
$\chi^2$ value	–	0.167	0.004	0.001	0	0	–	–	–
P value	–	0.682	0.950*	0.973*	1.000*	1.000*	0.509**	0.509**	0.509**

\* Was calculated using continuity correction; \*\* was calculated using the Fisher exact probability

observation group than in the control group ( $p < 0.05$ ), as seen in Table 4.

### Discussion

Anatomical abnormalities in the endonasal transsphenoidal approach are common in pituitary adenoma surgery. Lack of knowledge of the anatomical abnormalities leads to increased surgical complications and poor outcomes [16–18]. Studies

have shown that CT reconstruction and measurement techniques helped surgeons to solve practical problems during surgery and to accumulate experience for future operations.

The CT reconstruction of the nasal cavity and sphenoid sinus is significant for the removal of pituitary tumors. Reconstruction of anatomical structures in the nasal cavity can help surgeons to select the correct path for the surgical microscope, thus reducing unnecessary damage to the anatomical structure of the surgical approach. The CT reconstruction of sphenoid sinus can

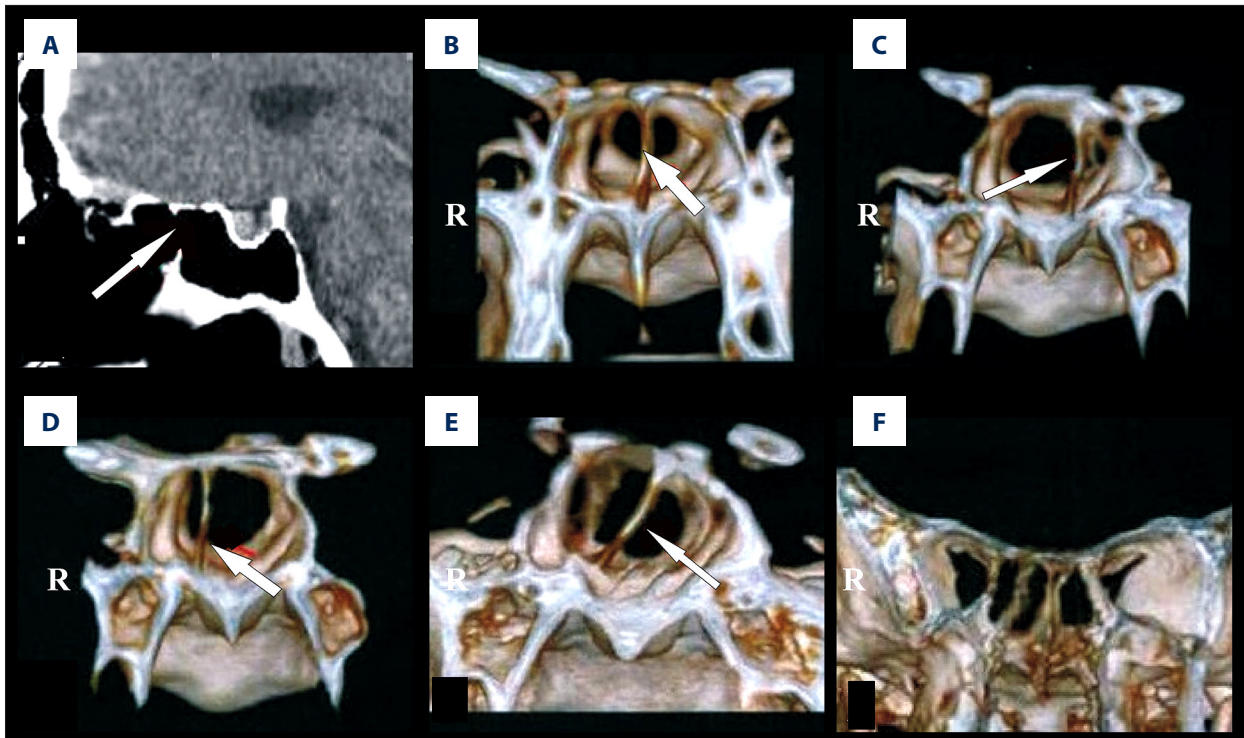


**Figure 3.** CT reconstruction and measurement of abnormal anatomy. (A) Three-dimensional (3-D) reconstruction images of the multi-atrial sphenoidal sinus septum. (B) Multiplanar reconstruction (MPR) sagittal measurement. OL is the skull base plane line. OP is the connection from the columella root to the sellar floor midpoint. OM is the connection from the columella root to the sphenoidal sinus inferior pole.



**Figure 4.** The MPR sagittal measurement of the lumen of the nasal sphenoidal region. OL is the skull base plane line. OP is the connection from the columella root to the sellar floor midpoint. OM is the connection from the columella root to the sphenoidal sinus inferior pole.

avoid the damage of the optic nerve in the suprasphenoidal cells and help surgeons choose the best way to remove the sphenoid interval, thus improving the efficacy of the operation and reducing the surgical complications.

The anatomical abnormalities in the endonasal transsphenoidal approach include nasal septal bending, middle turbinate pneumatization, middle turbinate reverse curvature, butterfly screening room, a sphenoid fissure, conchal sphenoid pneumatization, a sphenoid sinus septum, and bony defects in relation to the internal carotid artery. The normal position of the nasal septum is the middle of the nasal cavity, and its deviation to one side causes middle meatus stenosis. The middle turbinate is a solid structure and its volume increases after gasification, causing middle meatus stenosis. The abnormal bilateral middle turbinate bends inward, causing nasal meatus stenosis. CT reconstruction of abnormal structures can facilitate passage of the endoscope through the relatively wider middle meatus. When the endoscope moves through the narrow middle meatus without the help of CT-reconstructed images, repeated contact by the endoscope increases bleeding and damages the nasal mucosa. Recent studies have shown that patients with mucosal damage may experience postoperative complications such as voice change and anosmia [19,20]. Normally, the optic nerve is not wrapped in the ethmoid sinus above the sphenoid sinus unless anatomical abnormalities occur. MPR reconstruction reminder of operation evasion displays the precise position and anatomical structures and reduces injuries to the optic nerve.

**Table 3.** Comparisons of the postoperative complications between the observation group and the control group [case number (%)].

Groups	Cases	Cerebrospinal fluid leakage	Blood loss	Septum perforation	Diabetes insipidus	Infection	Sum
Observation group	26	1 (3.8)	0	0	1 (3.8)	0	2 (7.6)
Control group	27	4 (14.8)	2 (7.4)	2 (7.4)	2 (7.4)	1 (3.7)	11 (40.7)

**Table 4.** Comparisons of the perioperative indexes between the observation group and the control group ( $\bar{x}\pm s$ ).

Groups	Intraoperative blood loss (ml)	Operation time (min)	Postoperative hospital stay (d)
Observation group	50.0±8.4	97.6±9.0	5.0±1.6
Control group	80.4±7.3	155.0±15.7	7.4±1.1
<i>t</i> value	14.078	16.245	6.384
<i>P</i> value	<0.001	<0.001	<0.001

The aperture is a key area for entry into the sphenoid sinus during surgery. The sphenoid aperture is normally ovoid, but can present with different shapes when anatomical abnormalities are present. The base of the nasal columella is at a fixed position. Sharma et al. [21] demonstrated that the distance from the base of the columella to the inferior pole of the sphenoid sinus can provide the precise distance for the endoscope to reach the sphenoid sinus aperture, and is an accurate and reliable basis for reference. Conchal sphenoid sinus pneumatization is a relative contraindication to transsphenoidal surgery. Measurement of the sinus cavity can help predict the safety of the operation. Bony defects of the sphenoid posterior wall are occasionally found in patients with excess pneumatization in the sella of the saddle pillow type, which results in internal carotid artery exposure, with a prevalence of 10% [22]; this is a serious complication in pituitary adenoma resection [23]. In the present study, the prevalence was 3.7%. In the observation group, 1 patient with internal carotid artery exposure was detected by preoperative MPR, which enabled the surgeon to avoid serious complications. Proper removal of a sinus interval will provide optimal space for surgery, with single sinus interval completely removed and central sinus interval reserving a small part as the positioning mark, for which these operations can only be conducted around the middle to avoid injuring internal carotid arteries and the optic nerves, ensuring the safety of the operations. The size of sinus interval removal depends on the size of the operative space [24–26].

CT can provide accurate images and can help prevent complications [27–29]. Perioperative CT reconstruction and measurement can help reduce poor outcomes. Cerebrospinal fluid leakage was the most common complication observed in this study. The incidence in the observation group was 3.8%, while that in the control group was 14.8%. In recent years, the reported incidence has been below 5% [30–34]. The incidence in the observation group was lower than that in the above report, while that in the control group was higher. The comparative results of intraoperative blood loss, surgical time, and hospital stay showed that the observation group was superior to the control group, which was consistent with previous studies [35–38].

Our study has certain limitations due to its retrospective design and a relatively small sample size. In addition, the observations on nerves and vessels in the endonasal transsphenoidal approach were not sufficient, and the latest CT/MR image navigation technology was not used in this study.

## Conclusions

Our study demonstrates that CT reconstruction of the anatomical structure of pituitary tumor can avoid potential damage on nerves and blood vessels in patients with abnormal structures. Similarly, preoperative CT reconstruction and measurement of the abnormal structures in patients undergoing pituitary adenoma resection using the endonasal transsphenoidal approach can improve surgical quality and reduce complications.

## References:

1. Hardy J: Transsphenoidal microsurgery of the normal and pathological pituitary. *Clin Neurosurg*, 1969; 16: 185–217
2. Mehta GU, Lonser RR, Oldfield EH: The history of pituitary Surgery for Cushing disease. *J Neurosurg*, 2012; 116(2): 261–68
3. Tabaei A, Anand VK, Barton Y et al: Endoscopic pituitary surgery: A systematic review and meta-analysis. *J Neurosurg*, 2009; 111(3): 545–54
4. Esposito V, Santoro A, Minniti G et al: Transsphenoidal adenomectomy for GH-, PRL- and ACTH-secreting pituitary tumours: Outcome analysis in a series of 125 patients. *Neurophysiology*, 2004; 25: 251–56
5. Gondim JA, Schops M, de Almeida JP et al: Endoscopic endonasal transsphenoidal surgery: Surgical results of 228 pituitary adenomas treated in a pituitary center. *Pituitary*, 2010; 13(1): 68–77
6. Dhandapani S, Singh H, Negró HM et al: Cavernous sinus invasion in pituitary adenomas: Systematic review and pooled data meta-analysis of radiological criteria and comparison of endoscopic and microscopic surgery. *World Neurosurg*, 2016; 96: 36–46
7. Akin S, Isikay I, Sovlezmezoglu F et al: Reasons and results of endoscopic surgery for prolactinomas: 142 surgical cases. *Acta Neurochir (Wien)*, 2016; 158(5): 933–42
8. Ammirati M, Wei L, Ciric I: Short-term outcome of endoscopic versus microscopic pituitary adenoma surgery: A systematic review and meta-analysis. *J Neurol Neurosurg Psychiatry*, 2013; 84(8): 843–49
9. Xiangyu M, Xin Z, Weiguo L et al: Clinical research of endoscopic transsphenoidal surgery for pituitary adrenocorticotropic hormone adenoma. *Chin J Neurosurg*, 2014; 10(30): 1012–15
10. Mamelak AN, Carmichael J, Bonert VH et al: Single-surgeon fully endoscopic endonasal transsphenoidal surgery: Outcomes in three-hundred consecutive cases. *Pituitary*, 2013; 16(3): 393–401
11. Kim do H, Hong YK, Jeun SS et al: Anatomic. *Otolaryngol Head Neck Surg*, 2016; 154(6): 1132–37
12. Chabot JD, Chakraborty S, Imbarrato G et al: Evaluation of outcomes after endoscopic endonasal surgery for large and giant pituitary macroadenoma: A retrospective review of 39 consecutive patients. *World Neurosurg*, 2015; 84(4): 978–88
13. Zhengyi G, Ningxi Z: Effects of multiplanar reconstruction imaging on resection of pituitary tumor via transsphenoidal. *Chin J Digest Med Imageol (Electronic Edition)*, 2014; 2 (4): 21–23
14. Linsler S, Antes S, Senger S et al: The use of intraoperative computed tomography navigation in pituitary surgery promises a better intraoperative orientation in special cases. *J Neurosci Rural Pract*, 2016; 4(7): 598–602
15. Linsler S, Oertel J: Endoscopic endonasal transclival resection of a brainstem cavernoma: A detailed account of our technique and comparison with the literature. *World Neurosurg*, 2015; 6(84): 2064–71
16. Oertel J, Gaab MR, Linsler S: The endoscopic endonasal transsphenoidal approach to sellar lesions allows a high radicality: The benefit of angled optics. *Clin Neurol Neurosurg*, 2016; 146: 29–34
17. Kassam AB, Prevedello DM, Carrau RL et al: Endoscopic endonasal skull base surgery: Analysis of complications in the authors' initial 800 patients. *J Neurosurg*, 2016; 114(6): 1544–68
18. Linsler S, Oertel J: Endoscopic endonasal transclival resection of a brainstem cavernoma: A detailed account of our technique in comparison with the literature. *World Neurosurg*, 2015; 84(6): 2064–71
19. Kim BY, Shin JH, Kim SW et al: Hypernasality after using the endoscopic endonasal transsphenoidal approach for skull base tumors. *Laryngoscope*, 2016; 126(2): 329–33
20. Wenwen H, Yuping P: Recent advance in endoscopic transsphenoidal approach. *Chin J Neurosurg*, 2016; 6(15): 639–43
21. Sharma A, Dorman MF, Spahr AJ: A sensitive period for the development of the central auditory system in children with cochlear implants: Implications for age of implantation. *Ear Hear*, 2010; 23(6): 532–39
22. Rhoton AL: The sellar region. *Neurosurgery*, 2002; 51(4 Suppl.): S335–74
23. Kepron C, Cusimano M, Pollanen MS: Fatal hemorrhage following transsphenoidal resection of a pituitary adenoma: A case report and review of the literature. *Forensic Sci Med Pathol*, 2010; 6: 282–87
24. Berkman S, Schlaffer S, Nimsky C et al: Intraoperative high-field MRI for transsphenoidal reoperations of nonfunctioning pituitary adenoma. *J Neurosurg*, 2014; 121(5): 1166–75
25. Solari D, Cavallo LM, Somma T et al: Endoscopic endonasal approach in the management of Rathke's cleft cysts. *PLoS One*, 2015; 10(10): e0139609
26. Jiwei B, Chuzhong L, Songbai G et al: Comparison of endoscopic and microscopic transsphenoidal pituitary surgery. *Chin J Neurosurg*, 2015; 4 (31): 325–28
27. Walter T, Schwabe P, Schaser KD, Maurer M et al: Positive outcome after a small-caliber gunshot fracture of the upper cervical spine without neurovascular damage. *Pol J Radiol*, 2016; 81: 134–13
28. Kawai T, Ozawa Y, Ogawa M et al: Quality improvement of dual-energy lung perfusion image by reduction of low-energy X-ray spectrum: An evaluation on clinical images. *Pol J Radiol*, 2016; 81: 593–97
29. Abbas MS, AlBerawi MN, Al Bozom I et al: Unusual complication of pituitary macroadenoma: A case report and review. *Am J Case Rep*, 2016; 17: 707–11
30. Juraschka K, Khan OH, Godoy BL et al: Endoscopic endonasal transsphenoidal approach to large and giant pituitary adenomas: Institutional experience and predictors of extent of resection. *J Neurosurg*, 2014; 121(1): 75–83
31. Koutourousiou M, Gardner PA, Fernandez-Miranda JC et al: Endoscopic endonasal surgery for giant pituitary adenomas: Advantages and limitations. *J Neurosurg*, 2013; 118(3): 621–31
32. Gondim JA, Schops M, de Almeida JP et al: Endoscopic endonasal transsphenoidal surgery: Surgical results of 228 pituitary adenomas treated in a pituitary center. *Pituitary*, 2010; 13(1): 68–77
33. Zhao B, Wei YK, Li GL et al: Extended transsphenoidal approach for pituitary adenomas invading the anterior cranial base, cavernous sinus, and clivus: A single center experience with 126 consecutive cases. *J Neurosurg*, 2010; 112(1): 108–17
34. Ceylan S, Koc K, Anik I: Endoscopic endonasal transsphenoidal approach for pituitary adenomas invading the cavernous sinus. *J Neurosurg*, 2010; 112(1): 99–107
35. Dallapiazza R, Bond AE, Grober Y et al: Retrospective analysis of a concurrent series of microscopic versus endoscopic transsphenoidal surgeries for Knosp Grades 0-2 nonfunctioning pituitary macroadenomas at a single institution. *J Neurosurg*, 2014; 121(3): 511–17
36. Gao Y, Zhong C, Wang Y et al: Endoscopic versus microscopic transsphenoidal pituitary adenoma surgery: A meta-analysis. *World J Surg Oncol*, 2014; 12: 94
37. Dehdashti AR, Ganna A, Karabatsou K et al: Pure endoscopic endonasal approach for pituitary adenomas: Early surgical results in 200 patients and comparison with previous microsurgical series. *Neurosurgery*, 2008; 62(5): 1006–17
38. Rudmik L, Starreveld YP, Vandergriff WA et al: Cost-effectiveness of the endoscopic versus microscopic approach for pituitary adenoma resection. *Laryngoscope*, 2015; 125(1): 16–24